Available online at www.sciencedirect.com
ScienceDirect
Thin Solid Films 515 (2006) 1132–1137
thin solid films
www.elsevier.com/locate/tsf

Raman spectra and structural analysis in ZrO_xN_y thin films

C. Moura [a], P. Carvalho [b], F. Vaz [b], L. Cunha [a,*], E. Alves [c]

[a] Universidade do Minho, Dept. Física, Campus de Gualtar, 4710-057 Braga, Portugal
[b] Universidade do Minho, Dept. Física, Campus de Azurém, 4800-058 Guimarães, Portugal
[c] ITN, Departamento de Física, E.N.10, 2686-953 Sacavém, Portugal

Available online 7 September 2006

Abstract

Raman spectroscopy has been used as a local probe to characterize the structural evolution of magnetron-sputtered decorative zirconium oxynitride ZrO_xN_y films which result from an increase of reactive gas flow in the deposition. The lines shapes, the frequency position and widths of the Raman bands show a systematic change as a function of the reactive gas flow (a mixture of both oxygen and nitrogen). The as-deposited zirconium nitride film presents a Raman spectrum with the typical broadened bands, due to the disorder induced by N vacancies. The recorded Raman spectrum of the zirconium oxide film is typical of the monoclinic phase of ZrO_2, which is revealed also by X-ray diffraction. Raman spectra of zirconium oxynitride thin films present changes, which are found to be closely related with the oxygen content in films and the subsequent structural changes.

Keywords: Sputtering; Zirconium oxynitride; Raman; X-ray diffraction; Decorative coatings

1. Introduction

The metal oxynitrides, MeN_xO_y (Me = early transition metal), belong to a new class of materials that is gaining importance because of their high potential to be used for decorative applications in high quality consumer products. During last years there has been published work about the production and characterization of metal oxynitride thin films [1–7], but the understanding of the fundamental mechanisms that explain both structural and mechanical behaviour is yet insufficient. To prepare these films, very careful control of the gas flow rates is needed since the final properties will depend much on their atomic ratio, and oxygen exhibits a stronger reactivity than nitrogen with the metal [2].

Tuning the oxide/nitride ratio changes the crystallographic order between oxide and nitride, hence elucidating the relationship between the corresponding physical, structural and mechanical properties [6]. Most of the published work related with Raman scattering in zirconium oxide concerns dynamical properties [8–10], structural transformations induced by the additions of stabilizers [11–13] and nano-sized effects [14].

Zirconium oxide can be found basically in three different phases, cubic (c-ZrO_2), tetragonal (t-ZrO2) and monoclinic (m-ZrO_2). The structure of t-ZrO_2 belongs to the symmetry group $D_4^{15}{}_h$ ($P4_2/nmc$) with two units of ZrO_2 per unit cell, and 6 Raman active modes. Cubic zirconia belongs to the O_h^5 ($Fm\bar{3}m$) group with one unit of ZrO_2 per unit cell and only one Raman active mode, while the monoclinic structure belongs to the $D_2^5{}_h$ ($P2_1/c$) with four units of ZrO_2 per unit cell and 18 Raman active modes [10,15]. Many transition-metal nitrides, like ZrN, crystallise in the sodium-chloride-type structures and, in an ideal "perfect" crystal, first order Raman scattering is forbidden. Nevertheless sputtered coatings are known to have vacancies that induce distortion in the structure [7], and in consequence the Raman spectrum is composed of broadened bands due to disorder and second order processes.

The main purpose of this work is the preparation of single-layered zirconium oxynitrides, ZrO_xN_y films and the relationship between the composition and structure. Thin films, prepared by DC reactive magnetron sputtering, were characterized by Raman Spectroscopy (RS), and the results are correlated with the composition, evaluated by Rutherford Backscattering spectrometry (RBS), and the structure obtained by X-ray diffraction (XRD).

* Corresponding author. Tel.: +351 253 604 066; fax: +351 253 678 981.
E-mail address: lcunha@fisica.uminho.pt (L. Cunha).

0040-6090/$ - see front matter © 2006 Elsevier B.V. All rights reserved.
doi:10.1016/j.tsf.2006.07.039

2. Experimental details

ZrO_xN_y thin films were deposited onto high-speed steel (AISI M2), glass and single crystal silicon (100) substrates, by reactive dc magnetron sputtering. Details on film preparation conditions can be found elsewhere [6].

The atomic composition of the as-deposited samples was measured by Rutherford Backscattering Spectroscopy (RBS) using a 1.4 MeV He^+ beam and a 2 MeV proton beam to increase the accuracy in the oxygen signals. The analyzed area was about 0.5×0.5 mm^2. Ball crater tests were used to measure the thickness of the samples. In order to examine the film structure, X-ray diffraction experiments (XRD) were undertaken in a Philips PW 1710 apparatus, using Cu Kα radiation, with a step size of 0.02°, a counting time of 1.25°/s and a gas detector. Raman measurements were performed at room temperature with a Dilor triple monochromator, equipped with a liquid nitrogen cooled charge couple device (CCD) detector, with a resolution better than 1 cm^{-1}. The excitation line, 514.5 nm, of an argon ion laser was focused onto the sample using a ×100 MS Plan objective of an Olympus Microscope BHSM, in a backscattering geometry. The spectra were obtained with a measured power of about 10 mW on the sample, during an integration time of 120 s, over the range 80–1200 cm^{-1}.

3. Results and discussion

3.1. Chemical analysis

The samples thickness, measured by ball cratering, and the atomic composition determined by RBS are given in Table 1. A closer look of these results indicates three distinct zones of the composition of the thin films. The films deposited with reactive gas flow lower than 10 sccm present a non-metal to zirconium atomic ratio less than one, with a constant increase of the oxygen and nitrogen content. With further increase of the reactive gas flow (10–14 sccm) the samples present an (N+O)/Zr atomic ratio varying from 1.17 to 1.44 with further increases in the oxygen content resulting in approximately the same nitrogen content. For the sample deposited with the highest reactive gas flow (15 sccm), there is a stabilization of the non-metal to metal atomic ratio. When compared to the sample produced with a 14 sccm flow, a substantial increase in the oxygen content, is observed compared to samples prepared with lower gas flow. This evolution, observed for higher flow rates, with an abrupt increase in the oxygen content when the non-metal to metal atomic ratio is kept almost constant, suggests a change in the structural arrangement of the coatings, as we will discuss in this paper.

Table 1
Composition, thickness and non-metal to metal ratio $[(C_O+C_N)/C_{Zr}]$ of the samples prepared with different reactive gases flow rate

Sample	Gas flow (sccm)	Zr (at.%)	O (at.%)	N (at.%)	Thickness (μm)	Ratio $(C_O+C_N)/C_{Zr}$
$ZrO_{.05}N_{.49}$	6	65	≤3	32	3.1±0.4	0.49
$ZrO_{.05}N_{.67}$	7	58	≤3	39	2.8±0.3	0.67
$ZrO_{.09}N_{.79}$	8	53	5	42	2.8±0.5	0.89
$ZrO_{.10}N_{.83}$	9	52	5	43	3.5±0.3	0.92
$ZrO_{.20}N_{1.02}$	10	45	9	46	4.3±0.4	1.22
$ZrO_{.26}N_{.91}$	11	46	12	42	3.2±0.4	1.17
$ZrO_{.28}N_{1.05}$	12	43	12	45	3.9±0.6	1.33
$ZrO_{.37}N_{.95}$	13	43	16	41	3.4±0.5	1.33
$ZrO_{.37}N_{1.07}$	14	41	15	44	6.2±0.5	1.44
$ZrO_{.73}N_{.71}$	15	41	30	29	3.3±0.4	1.44

3.2. X-ray diffraction

In order to understand the mechanism of structure evolution with variation of the reactive gas flow, X-ray diffraction (XRD) analysis was carried out. Fig. 1 shows the X-ray diffraction patterns for samples prepared with increasing reactive gas flow. From the obtained diffraction patterns, it is possible to observe the formation of three different types of structures. The first of these zones corresponds to the films prepared with gas mixture flows varying from 6 to 10 sccm, will be noted in the text as zone I, developed a face centred cubic ZrN type structure.

For higher gas mixture flows, a change in structure occurs and a second zone, indexed as zone T, is developed. This second zone is what one might call a transition zone, whose diffraction patterns (very reduced and difficult to index) revealed the possibility of having the formation of poorly crystallized oxygen-doped orthorhombic, Zr_3N_4-type structures [6,7,16–19].

For the highest flows there is another structural change, revealing the development of a third zone, which will be referred throughout the text as Zone II, corresponding to films that the diffraction patterns (again very reduced and quite difficult to index) might indicate the preparation of films that crystallize in a zirconium oxynitride-type structure. The exact nature of this possible oxynitride structure is not yet accurately determined.

Furthermore, by comparing the evolution of the diffraction data of the oxynitride films prepared with low gas flows (from 6 to 8 sccm), it is possible to observe some texture change, decreasing the dominant <111> growth to approximately randomly oriented crystals, with the fcc-ZrN structure. This change could be associated with the increase of nitrogen content of the sub-stoichiometric fcc-ZrN structures (see Table 1).

For the films prepared with reactive gas flows higher than 10 sccm (zone T), the results of composition analysis revealed the presence of over-stoichiometric films, where the non-metal to metal atomic ratio varies from 1.17 to 1.44 (Table 1), and thus indicating the possibility to form different crystalline structures beyond the previously mentioned ZrN films. The sample prepared with a gas flow of 10 sccm seems to present already another phase, which is evident in the large broad peak around $2\theta = 30°$, becoming even more pronounced in the sample prepared with 13 sccm (Fig. 1). For this sample, the diffraction data reveals also a broad peak located at $2\theta \approx 32.2°$. The broadening of the peak at $2\theta \approx 32.2°$, which would correspond to the (320) plane of the o-Zr_3N_4 structure, could result from the small grain size and/or some reduction of the crystalline volume fraction of the coating, or even to a superposition of several peaks predicted in this region for this structure. The indexation of a particular crystalline structure to this sample is very difficult to fulfil due to the reduced number of diffraction peaks,

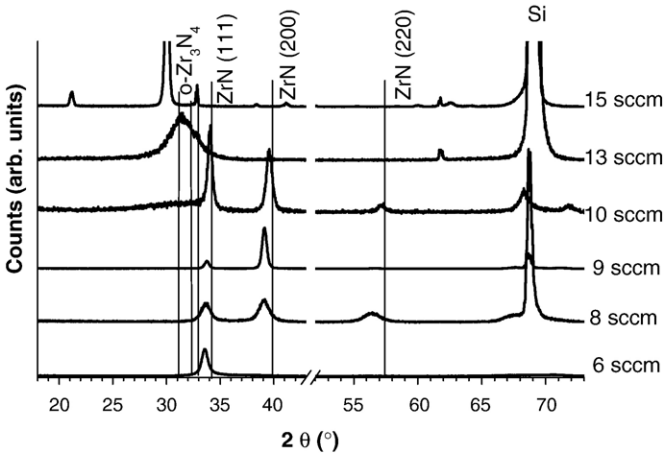

Fig. 1. XRD diffraction patterns of ZrO_xN_y films for different reactive gases flow rates.

although the available literature data suggest the formation of a structure very similar to that of Zr_3N_4-type, but with possible oxygen inclusions [16]. This change is also confirmed by the composition data, with the abrupt increase of the concentration of non-metallic elements. Looking into Table 1 it is possible to observe that the samples deposited with reactive gas flow varying from 10 to 13 sccm, present a concentration of the non metallic elements that varies from 1.22 to 1.33, which in fact is very close to the stoichiometric value of a Zr_3N_4-type structure. With a continuous increase of the reactive gas (higher than 14 sccm), there is another structure change, zone II. This structural change is well correlated with the evolution of the oxygen and nitrogen content of the coatings (Table 1). The semi-transparent sample, deposited with 15 sccm, shows a significant increase of the oxygen content along with a significant decrease of the nitrogen and its stoichiometry could correspond to an oxynitride-type structure. However, the exact determination of the crystalline structure is again very difficult due the reduced number of visible diffraction peaks. Nevertheless, and according to very few research studies [19–22] the diffraction peaks located at $2\theta \approx 21.1°$, $2\theta \approx 30°$ and $2\theta \approx 32.9°$ could correspond to a bcc γ-Zr_2ON_2-type structure (ICDD card n° 48-1635) [23].

3.3. Raman spectra

To correlate the changes in Raman spectra of all samples, each spectrum was normalized to the total scattering intensity. To analyse the changes due the deposition parameters, the "true" line shape of the spectra must be found. To recover this line shape, the position and the widths of the scattered bands, a least squares best fit with five Lorentzian profiles was performed.

In order to compare the evolution of structural modifications in ZrO_xN_y samples, the spectra of ZrN and ZrO_2, deposited in the same chamber, are depicted in Fig. 2a and b, respectively. In zirconium nitride, first order Raman scattering is forbidden as a consequence of selection rules. However due to disorder, induced by the deposition technique, the translation symmetry is lost, and thus all the modes can participate in the scattering. Raman spectra will be an "image" of the density of vibrational

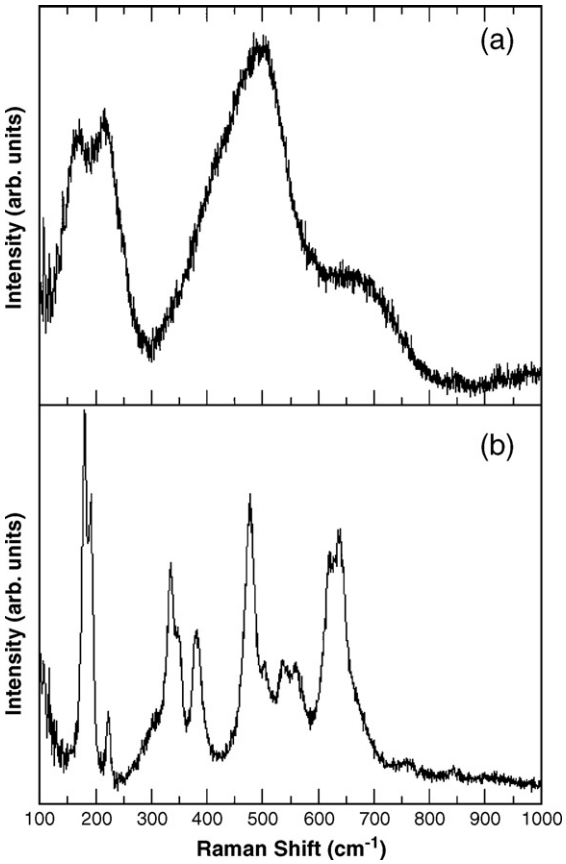

Fig. 2. Raman spectra: (a) Zirconium Nitride; (b) Zirconium Oxide.

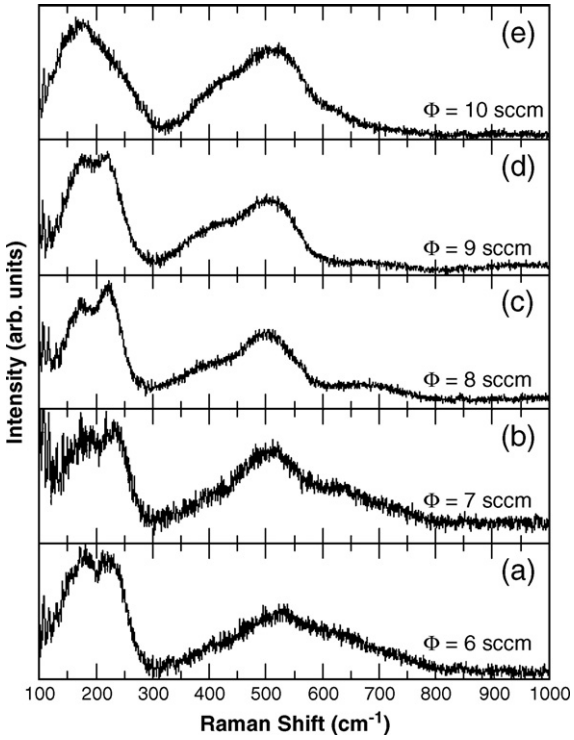

Fig. 3. Raman spectra of films as a function of reactive gases flow rate, from 6 to 10 sccm.

states (DVS) [24]. The Raman spectrum of ZrN, as expected, is dominated by an asymmetric band centred at around 500 cm^{-1}, and in the low frequency region by the presence of two bands centred at around 165 and 220 cm^{-1}, reflecting the material's DVS. In the low frequency range, the bands are attributed to the disorder of single phonons and second order processes. For higher frequencies the presence, and the asymmetry, of the bands is due to the superposed contributions of disorder of optical phonons and second order combination of acoustic and optical processes [25].

The spectrum of as-deposited zirconia, ZrO_2, is depicted in Fig. 2b, and is formed by several peaks, well defined, that can be identified as the characteristic features of the Raman spectrum of zirconia's monoclinic phase [14,26,27]. Even if the deposited sample is not a perfect crystal and even if some of the features are not very well resolved, it is noted that 16 of the 18 theoretical calculated features for the m-ZrO_2 phase are present [10].

In Figs. 3 and 4, the Raman spectra of the coatings deposited with increasing reactive gas flow are presented. The analysis of the evolution of the Raman signal, with the variation of gases flow, will be centered on two aspects: the first one will be the changes in the spectral shapes; the second a quantitative analysis based on band or peak position and the relative intensities of some of the detected peaks. As can be seen from these figures, with the variation of gas flow (in fact inducing the variation of the non metallic content) the lines shapes continuously change, and the appearance of new bands in spectra reflects the changes in composition and, consequently, in the structure. The absence of sharp and well defined peaks could be attributed to the local structural disorder of the prepared films.

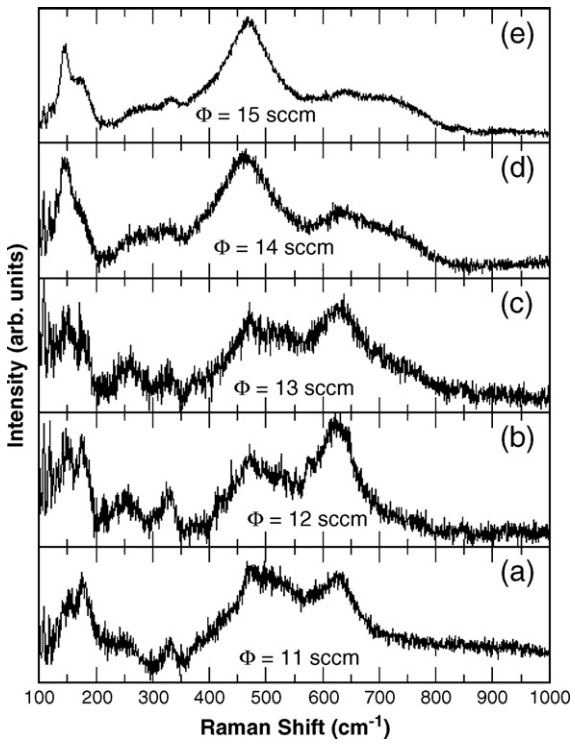

Fig. 4. Raman spectra of films as function of reactive gases flow rate, from 11 to 15 sccm.

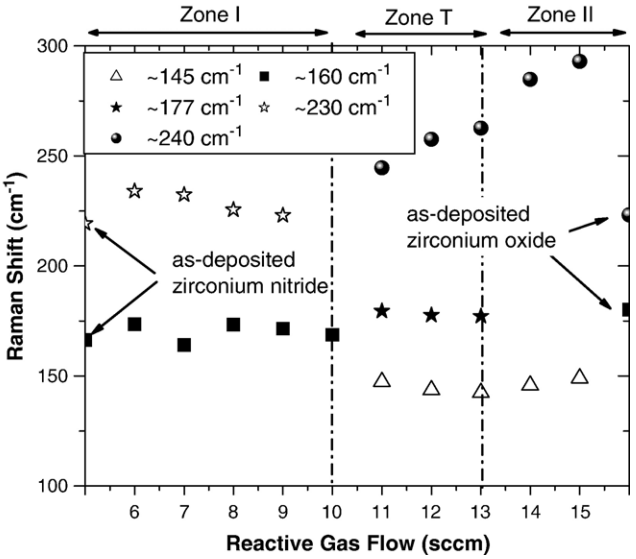

Fig. 5. Variation of the Raman shift of low frequency bands, as function of reactive gases flow rate.

The first note is that the spectral shape of Fig. 3a and b presents some similarities to spectrum of zirconium nitride. It is clearly seen that in the region below 300 cm^{-1}, two bands occur, which possess positions close to the bands observed in the spectrum of as-deposited ZrN. For frequencies higher than 300 cm^{-1}, the presence of a large band extended up to frequencies around 800 cm^{-1} is noticed, with lower intensity when compared with the band in the as-deposited ZrN spectrum [see Fig. 2a]. With the increase of the oxygen content, the spectral shape continues to change: a shoulder located at around 420 cm^{-1} starts to appear, as can be seen in Fig. 3d − e. The overlap of low frequency range features is also observed for flow rates around 10 sccm, as it can be seen in spectrum of Fig. 3e, and the transformation to a asymmetrical band centered at ~170 cm^{-1}. A considerable modification of the spectral shape occurs for flow rates higher than 10 sccm, as can be seen in spectra depicted in Fig. 4, where the number of visible bands increases: the appearance of new bands in the region between 200 and 300 cm^{-1}, and also in the region between 400 and 700 cm^{-1}. For flow rates higher then 13 sccm, another modification of the spectral shape is observed. In the present case, the reduced number of visible Raman bands seems closely related to the overlap of bands in the region between 200 and 400 cm^{-1} and the decrease in intensity of the band located at 640 cm^{-1}. In consequence the spectra are dominated by a large band centered around 460 cm^{-1}. In all the spectra presented in Fig. 4, some of the features appear in positions close to the expected frequencies of modes belonging to monoclinic and tetragonal phases of zirconium oxide. On the other hand, the presence of broad bands, indicative of local disorder, could be due to a non-stoichiometric phase of ZrO_xN_y-type structure and to a poorly crystallized Zr_3N_4 structure, as discussed in XRD results. All these changes reflect modifications in local arrangements that lead to the conclusion that the increase of oxygen fraction induces the formation of new structural arrangements. This observation will be later discussed.

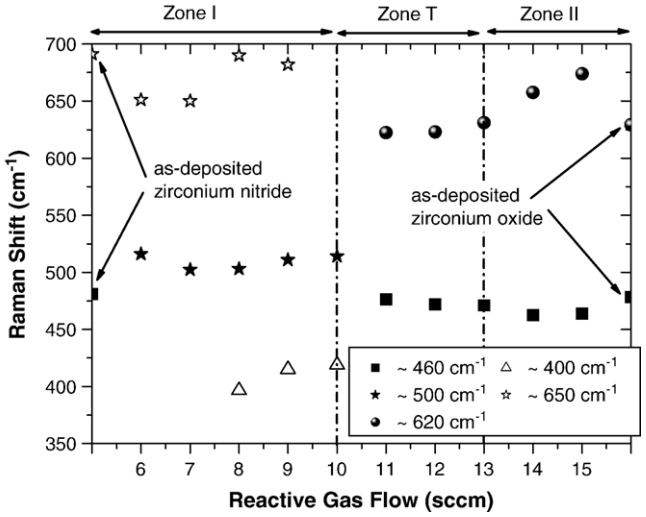

Fig. 6. Variation of the Raman shift of high frequency bands, as function of reactive gases flow rate.

In order to clarify the changes induced by the deposition conditions, in Figs. 5 and 6 are depicted the fittings results of the position for some bands, which have been chosen to perform a qualitative study: two bands situated in the low frequency range, centered around 167 and 220 cm^{-1}; and two bands situated at higher frequencies, centered around 475 and 680 cm^{-1}.

As can be seen in both figures, it is possible to divide the evolution of the band position in three zones, and correlate the observed behaviour with the observations that have been discussed for XRD-results. The observed shifts in band position could be attributed to film stresses, to non-stoichiometry of the deposited films and to changes in local structural arrangements, resulting from the deposition conditions itself.

A shift, to low frequency positions, is observed in the bands of the first region with the increase of flow rate. Incorporation of either O atoms into Zr nitride lattice, or N atoms in Zr oxide, in interstitial sites or by substitution, is expected. In spite of the fact that oxygen is more reactive than nitrogen, the nitrogen fraction in the working atmosphere is much more important than the oxygen and, obviously, this fact has consequences in the resulting structural evolution. As already discussed, the displayed spectra, for samples deposited with flow rates up to 7 sccm (in region zirconium nitride-like), are very similar to the as-deposited zirconium nitride sample. With the increase of oxygen content in the films, that increases at an almost constant rate as has been seen by RBS results, some incorporation of oxygen in zirconium nitride lattice is expected, or the substitution of nitrogen atoms by oxygen ones, and consequently the appearance of new bands in Raman spectra: the shoulder located at ~400 cm^{-1} and a large band located at ~690 cm^{-1} (see Fig. 4). These bands are present for flow rates higher than 8 sccm, but they vanish for flow rates equal to 10 sccm. The effect of oxygen content on Raman spectra is clearly seen in zone T and zone II, where the number of observed bands is higher than those observed in spectra of films of zone I. The observed shifts for the bands located at ~240 and ~480 cm^{-1}, to higher and low frequency respectively could not be attributed only to compressive stress, but also to lattice dynamics. In fact the changes in local structural arrangements observed in t-ZrO_2 samples were correlated to changes in tetragonality [28]. Some of the band positions, approach the characteristic positions of m-ZrO_2 ant t-ZrO_2 indicating the possible coexistence of these phases with a ZrO_xN_y-type structure.

4. Conclusions

Thin Zr–O–N films were prepared by dc reactive magnetron sputtering. Structural analysis carried out by both XRD and Raman revealed a definite correlation of the obtained results with the composition analysis, implying the existence of 3 different structural regimes. The first, zone I, corresponded to films prepared with the lowest reactive gas flows, present a zirconium nitride type structure. For the highest flows, a second zone was observed, zone II, and the XRD results show the possibility to have a bcc γ-Zr_2ON_2-type structure. Between these two zones, there is a transition zone, whose diffraction patterns revealed the possibility of having the formation of very poorly crystallized oxygen-doped orthorhombic Zr_3N_4-type structure. The Raman line shapes continuously change with the variation of the material composition. The observed changes reflect the modifications in local arrangements induced by the increase of oxygen fraction in the films. The appearance of new bands in spectra reflect also the changes in the local structure, induced by the particular composition of the samples. The XRD results, associated with Raman data, revealed the possibility of coexistence of different phases.

Acknowledgements

The work described in this paper is supported by the European Union through the NMP3-CT-2003 505948 project “HARDECOAT”. The authors are also grateful to the financial support of the Portuguese FCT institution by the project n° POCTI/CTM/38086/2001 co-financed by the European community fund FEDER and to Dr. A. Zwick for the helpful discussion about Raman data.

References

[1] R. Fraunchy, Surf. Sci. Rep. 38 (2000) 195.
[2] N. Martin, O. Banakh, A.M.E. Santo, S. Springer, R. Sanjinés, J. Takadoum, F. Lévy, Appl. Surf. Sci. 185 (2001) 123.
[3] F. Vaz, P. Cerqueira, L. Rebouta, S.M.C. Nascimento, E. Alves, Ph. Goudeau, J.P. Rivière, Surf. Coat. Technol. 174 – 175 (2003) 197.
[4] F. Vaz, P. Cerqueira, L. Rebouta, S.M.C. Nascimento, E. Alves, Ph. Goudeau, J.P. Rivière, K. Pischow, J. de Rijk, Thin Solid Films 447 – 448 (2004) 449.
[5] J. Barbosa, L. Cunha, L. Rebouta, C. Moura, F. Vaz, S. Carvalho, E. Alves, E. Le Bourhis, Ph. Goudeau, J.P. Rivière, Thin Solid Films 494 (2006) 201.
[6] P. Carvalho, F. Vaz, L. Rebouta, L. Cunha, C.J. Tavares, C. Moura, E. Alves, A. Cavaleiro, Ph. Goudeau, E. Le Bourhis, J.P. Rivière, J.F. Pierson, O. Banakh, J. Appl. Phys. 98 (2005) 023715.
[7] F. Vaz, P. Carvalho, L. Cunha, L. Rebouta, C. Moura, E. Alves, A.R. Ramos, A. Cavaleiro, Ph. Goudeau, J.P. Rivière, Thin Solid Films 469–470 (2004) 11.
[8] G.M. Rignanese, F. Detraux, X. Gonze, A. Pasquarello, Phys. Rev., B 64 (2001) 134301.

[9] A. Cros, A. Cantarero, D. Beltrán-Porter, J. Oró-Solé, A. Fuertes, Phys. Rev., B 67 (2003) 104502.
[10] A.P. Mirgorodsky, M.B. Smirnov, P.E. Quintard, J. Phys. Chem. Solids 60 (1999) 985.
[11] C.G. Kontoyannis, G. Carountzos, J. Am. Ceram. Soc. 77 (1994) 2191.
[12] D.J. Kim, H.J. Jung, J. Am. Ceram. Soc. 76 (1993) 2106.
[13] D.J. Kim, H.J. Jung, H.L. Lee, J. Am. Ceram. Soc. 80 (1997) 1453.
[14] M. Jouanne, J.F. Morhange, M.A. Kanehisa, E. Haro-Poniatowski, G.A. Fuentes, E. Torres, E. Henández-Telles, Phys. Rev., B 64 (2001) 155404.
[15] B. Králik, E.K. Chang, S.G. Louie, Phys. Rev., B 57 (1998) 7027.
[16] D.I. Bazhanov, A.A. Knizhnik, A.A. Safonov, A.A. Bagatur'yants, M.W. Stoker, A.A. Korkin, J. Appl. Phys. 97 (2005) 044108.
[17] J.P. Dauchot, S. Edart, M. Wautelet, M. Hecq, Vacuum 46 (1995) 927.
[18] B.O. Johansson, H.T.G. Hentzell, J.M.E. Harper, J.J. Cuomo, J. Mater. Res. 1 (1986) 442.
[19] L. Pichon, T. Girardeau, A. Straboni, F. Lignou, P. Guérin, J. Perrière, Appl. Surf. Sci. 150 (1999) 115.
[20] M. Lerch, J. Mater. Sci. Lett. 17 (1998) 441.
[21] H. Wiame, M.-A. Centeno, S. Picard, P. Bastians, P. Grange, J. Eur. Ceram. Soc. 18 (1998) 1293.
[22] I. Milosev, H.H. Strehblow, M. Gaberscek, B. Navinsek, Surf. Interface Anal. 24 (1996) 448.
[23] S.J. Clarke, C.W. Michie, M.J. Rosseinsky, J. Solid State Chem. 146 (1999) 399.
[24] A.N. Christensen, O.W. Dietrich, W. Kress, W.D. Teuchert, Phys. Rev., B 19 (1979) 5699.
[25] A. Cassinese, M. Iavarone, R. Vaglio, M. Grimsditch, S. Uran, Phys. Rev., B 62 (2000) 13915.
[26] B.K. Kim, H. Hamaguchi, Phys. Status Solidi 203 (1997) 557.
[27] P. Barberis, T. Merle-Méjen, P. Quintard, J. Nucl. Mater. 246 (1997) 232.
[28] P. Barberis, G. Corolleur-Thomas, R. Guinebretière, T. Merle-Méjen, A. Mirgorodsky, P. Quintard, J. Nucl. Mater. 288 (2001) 241.